Supplementary materials for
Impact of the isoprene photochemical cascade on tropical ozone

F. Paulot, D. K. Henze and P. O. Wennberg

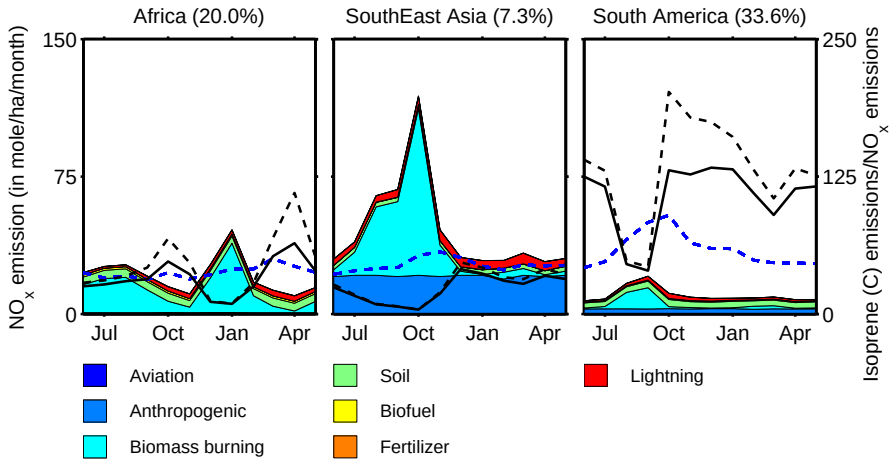

Figure S1: The three continental regions considered in this study (Fig. 1) account together for $\sim 60\%$ of isoprene global emissions (geographical breakdown is indicated in the panels' title). Very different NO_x/isoprene regimes (black line for NO_x/isoprene and dashed black line for $NO_x^{surface}$/isoprene) and NO_x sources (colored regions) are experienced through the year with South America C(isoprene)/N emissions exceeding 50 for most of the year. The seasonality of the ratio of isoprene emissions to NO_x emissions is primarily controlled by biomass burning, as seasonal variations of isoprene emissions (dashed blue line, in mole of C/ha/month $\times 1/25$, left axis) are small. The ratio of NO_x emissions to isoprene emissions is weighted by isoprene emissions to represent the average NO_x encountered by isoprene.

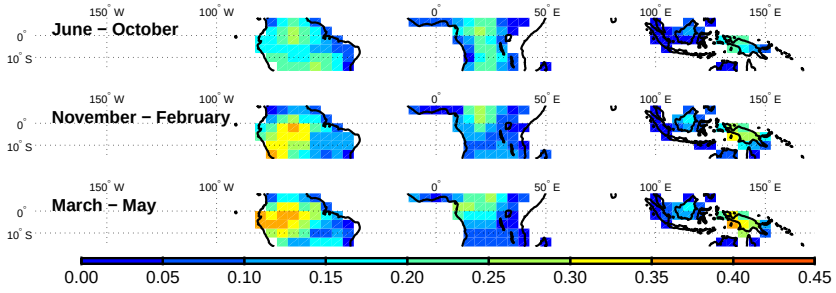

Figure S2: Fraction of isoprene oxidized above 800 mbar. About 20% of isoprene is predicted to be oxidized outside of the boundary layer in the tropics.

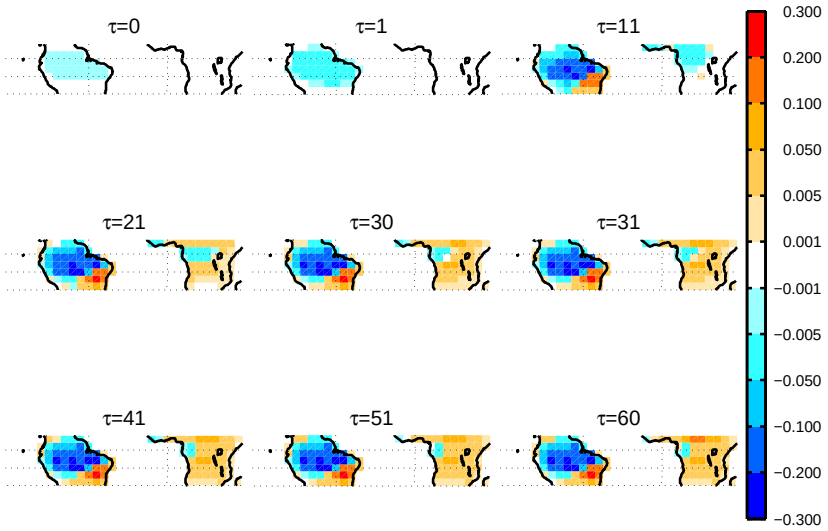

Figure S3: Sensitivity of ozone over South America (${}^{\mathrm{S}}\mathcal{S}^{\mathrm{O_3}}_{\mathrm{E(ISOP)}}$ in ‰/$\circ^2$) evaluated from May 31 to June 1, for different buffer times (τ in days).

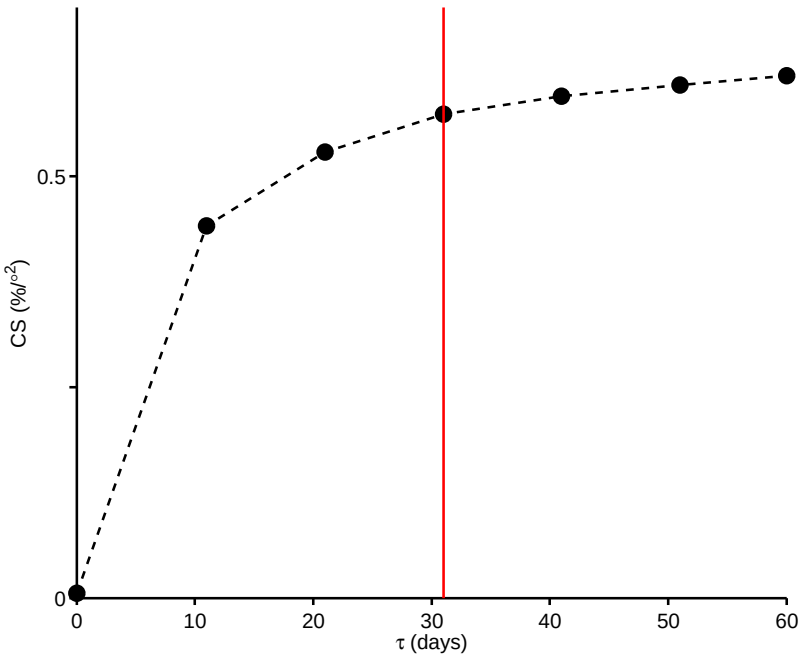

Figure S4: Cumulative sensitivity of ozone over South America ($CS = \sum_{i \in t} \left| {}^{\mathrm{S}}_{\mathrm{i}} \mathcal{S}^{\mathrm{O_3}}_{\mathrm{E(ISOP)}} \right|^2$) from May 31 to June 1, for different buffer time (τ). The vertical red line indicates the buffer integration time used in the simulations.

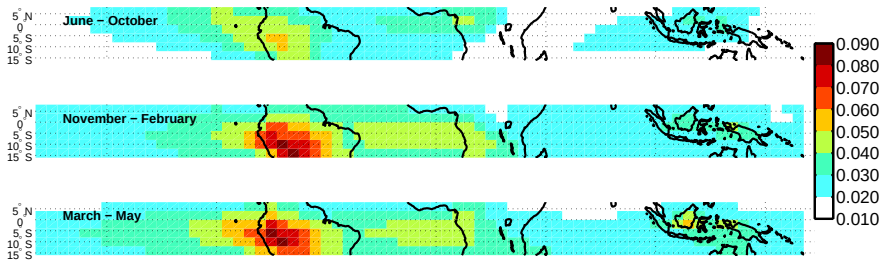

Figure S5: The representation of isoprene nitrate chemistry directly impacts simulated tropical ozone, as illustrated by the normalized standard deviation in the simulated ozone tropospheric column for different choices of nitrate yield (Y), NO_x recycling (α) and ING deposition (excluding Y=0% and Y=10% with no ING chemistry). The choice of the representation of isoprene nitrate chemistry is most important outside of the biomass burning seasons and affects large regions of the tropics. Conversely, changes in the representation of isoprene nitrate chemistry causes little change in regions affected by biomass burning.

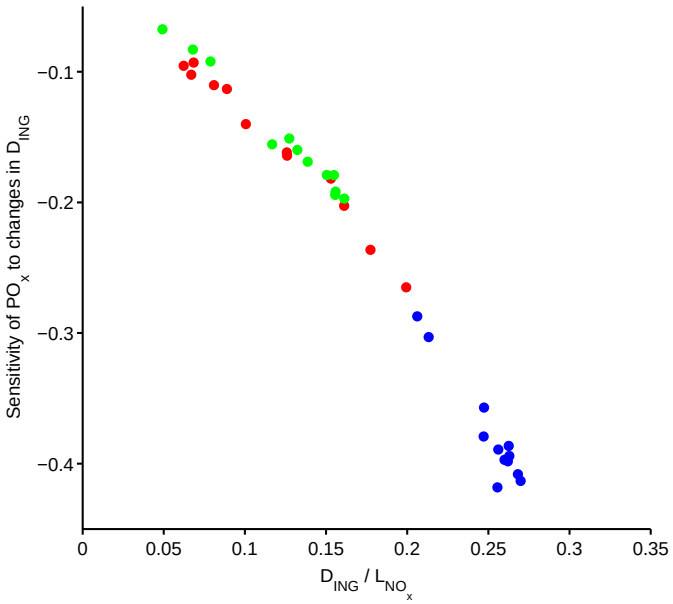

Figure S6: The sensitivity of $\mathcal{P}_{\mathrm{O_x}}$ to the representation of isoprene nitrate chemistry is well explained by the fraction of $\mathrm{NO_x}$ removed through ING chemistry ($\mathcal{D}_{\mathrm{ING}}/\mathcal{L}_{\mathrm{NO_x}}$). Red: Africa, blue: South America, green: South East Asia

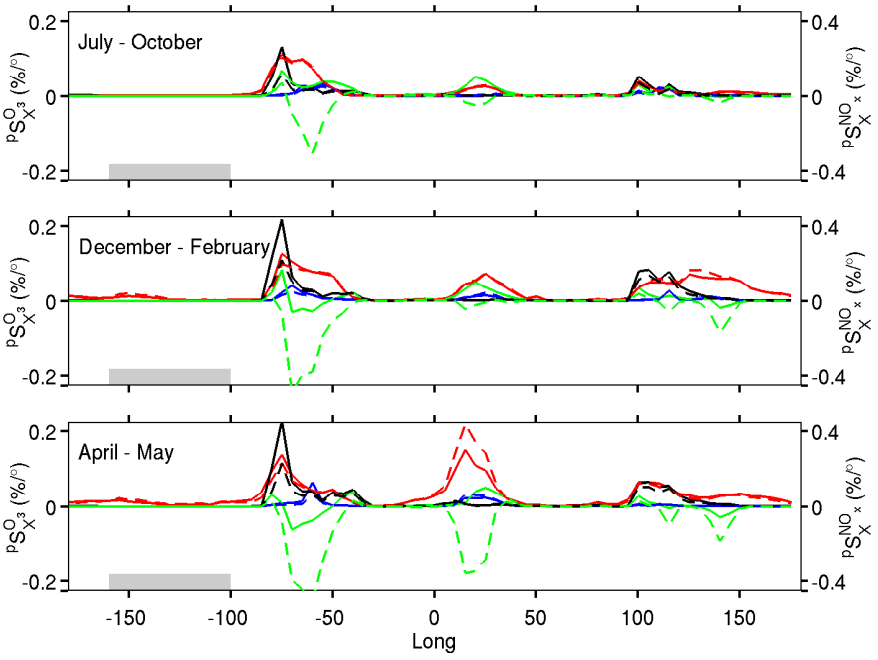

Figure S7: Adjoint sensitivity of tropospheric ozone (solid line) and NO_x (dashed line) over the Pacific (shaded region) to changes in the emissions of isoprene (green), lightning NO_x (red, $\times 0.5$), biomass burning NO_x (blue) and anthropogenic NO_x (black). The grey shaded region denotes the region over which the cost functions are evaluated.

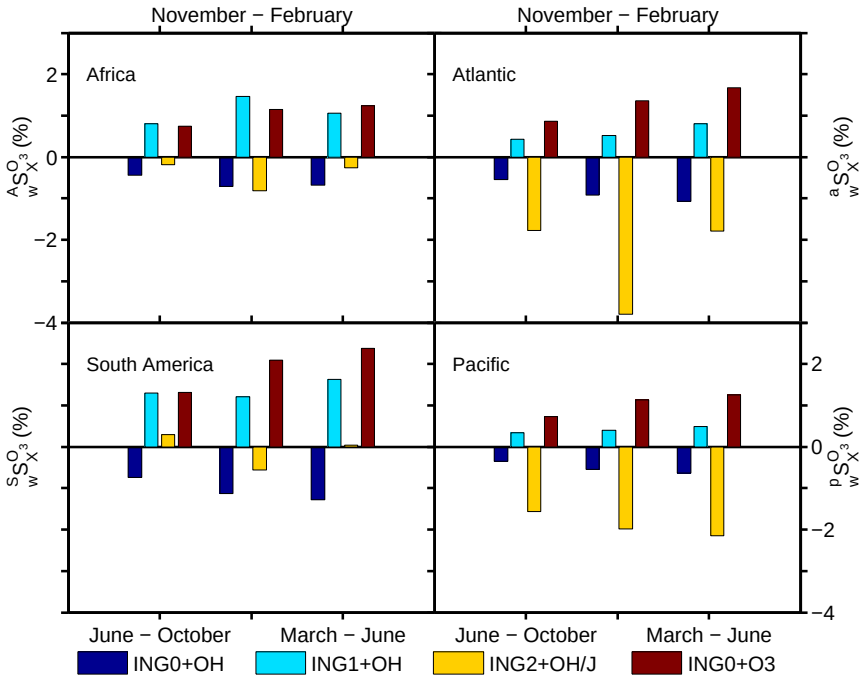

Figure S8: The sensitivity of tropospheric ozone to changes in key reactions controlling the fate of ING_0, ING_1 and ING_2 exhibits strong seasonal and regional differences. Faster oxidation of ING_0 and ING_1 are associated with higher ozone in particular over continental regions where NO_x is limited (e.g., South America from March to June). Here, ${}_{w}\mathcal{S}^{O_3} = \sum_{\forall x} {}_{x}s^{O_3}$.

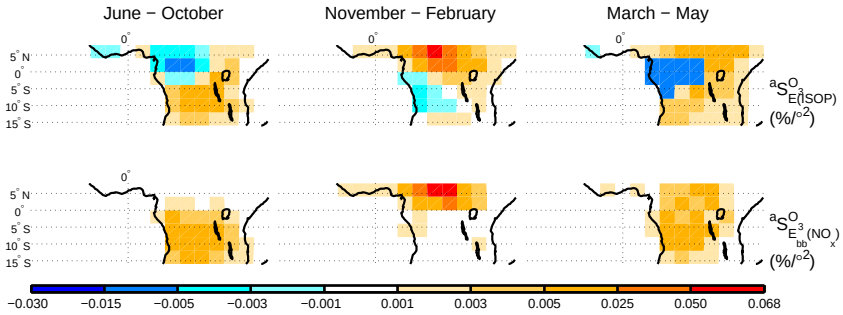

Figure S9: Adjoint sensitivity of Atlantic ozone to emissions of isoprene (top panels) and NO_x from biomass.

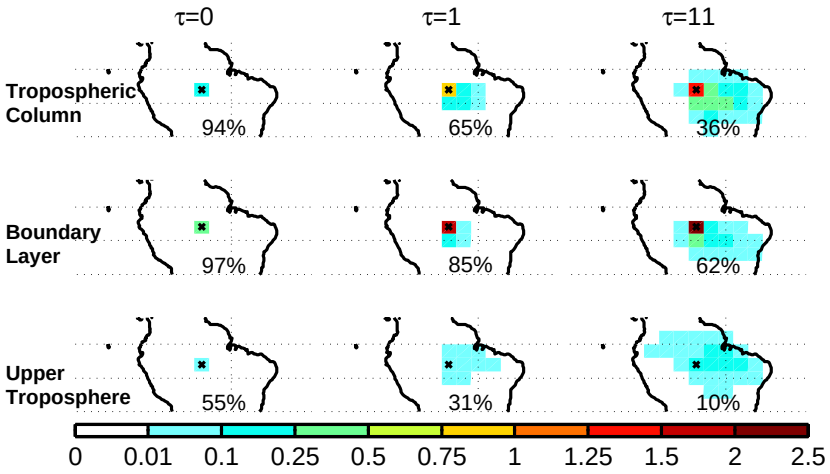

Figure S10: The sensitivity of formaldehyde to isoprene emissions calculated with the adjoint reveals the large spatial and temporal footprint of isoprene emissions on formaldehyde in the GEOS-Chem model. Adjoint sensitivities of tropospheric, boundary layer and upper tropospheric formaldehyde partial columns to changes in isoprene emissions (in $\%/\circ^2$) are calculated for one grid cell ($4^\circ \times 5^\circ$) at -6°N, 60°W (denoted by a cross) from May 31 to June 1 for different buffer times (τ in days). The fraction of the overall sensitivity due to isoprene emissions in the -6°N, 60°W box indicated in %.

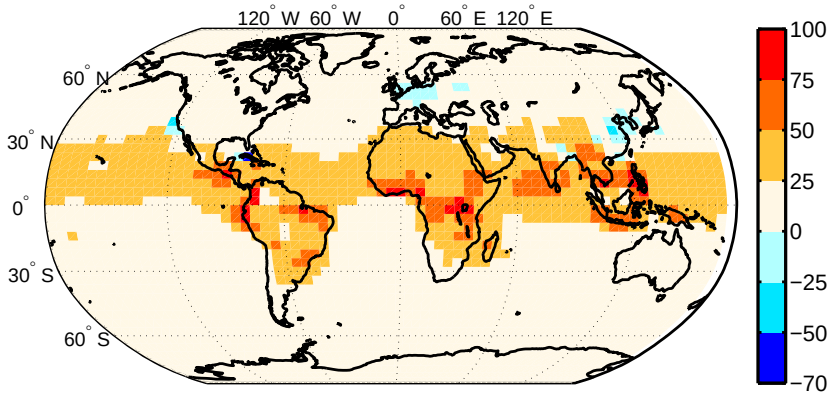

Figure S11: Relative change (in %) in the tropospheric ozone column as NO_x emissions are set to North America mean NO_x emission per capita (see text).

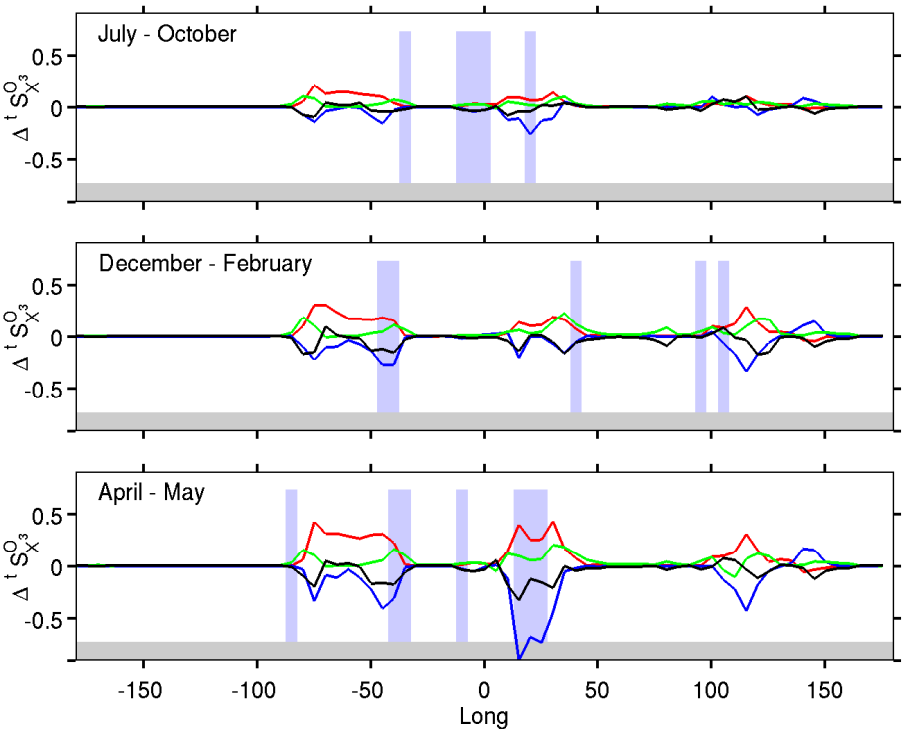

Figure S12: Absolute changes in the adjoint sensitivity of tropospheric tropical ozone ($\Delta^{t}\mathcal{S}_{X}^{O_3}$=($^{t}\mathcal{S}_{X}^{O_3}$(H − NO_x) − $^{t}\mathcal{S}_{X}^{O_3}$)×100, with $^{t}\mathcal{S}_{X}^{O_3}$ in $\%/\circ^2$) to changes in the isoprene nitrate yield (red), the isoprene nitrate recycling (blue, ×5), the loss rate of methane (green, $CH_4 + OH$), the rate of $OH + NO_2$ (black, ×0.5) resulting from a very large increase in NO_x emissions. Adjoint sensitivities are summed over the entire troposphere from -15°N to 7°N. Blue-shaded areas denote regions where $^{t}\mathcal{S}_{X}^{O_3}$ become negative because of higher NO_x emissions.

Table S1: Summary of the changes to the standard GEOS-Chem mechanism

$ISOP + OH$	$\rightarrow$	$ISOPO2$	$2.7 \times 10^{-11} \times \exp(390/T)$
$ISOPO_2$	$\rightarrow$	$OH + 2\,HO_2 + CH_2O$+0.5(MGLY + GLYC + GLYX + HAC)	$4.07 \times 10^{8} \times \exp(-7694/T)$
$ISOPO_2 + NO$	$\rightarrow$	$NO_2 + HO_2$+0.378IALD+ +0.378MVK+0.244MACR + $0.622CH_2O$	$(1-Y) \times k_{NO}$[b]
$ISOPO2 + NO$	$\rightarrow$	ING0	$Y \times k_{NO}$[b]
$ING_0 + OH$	$\rightarrow$	$ING0O_2$	$1.28 \times 10^{-11} \times \exp(380/T)$
$ING_0O_2 + NO$	$\rightarrow$	$2NO_2 + HO_2$ + OVOC	$\alpha \times 2.7 \times 10^{-12} \times \exp(350/T)$
$ING_0O_2 + NO$	$\rightarrow$	$0.5ING_1$+$0.5ING_2$ + HO_2 + NO_2	$(1-\alpha) \times 2.7 \times 10^{-12} \times \exp(350/T)$
$ING_0O_2 + HO_2$	$\rightarrow$		k_{HO_2}[a]
$ING_0 + O_3$	$\rightarrow$	NO_2 + HO_2 + OVOC	$\alpha \times 1.09 \times 10^{-13} \times \exp(-2100/T)$
$ING_0 + O_3$	$\rightarrow$	$0.5ING_1$+$0.5ING_2 + HO_2$	$(1-\alpha) \times 1.09 \times 10^{-13} \times \exp(-2100/T)$
$ISOP + NO_3$	$\rightarrow$	INO_2	$3.15 \times 10^{-12} \times \exp(-450/T)$
$MVK + OH$	$\rightarrow$	$MVKO_2$	$2.6 \times 10^{-12} \exp(610/T)$
$MVKO_2 + NO$	$\rightarrow$	NO_2+ $0.28HO_2$ + OVOC	k_{NO}[b]
$MVKO_2 + NO$	$\rightarrow$	ING_1	k_{NO}[b]
$MACR + OH$	$\rightarrow$	$MRO_2 + MAO_3$	k_{NO}[b]
$MRO_2 + NO$	$\rightarrow$	$NO_2 + OH$	k_{NO}[b]
$MRO_2 + NO$	$\rightarrow$	ING_1	k_{NO}[b]
$INO_2 + NO$	$\rightarrow$	$1.15NO_2 + 0.8HO_2 + 0.85ING_0 + 0.1$MACR $0.15CH_2O + 0.05$MVK	k_{NO}[b]
$INO_2 + HO_2$	$\rightarrow$	INPN	k_{HO_2}[a]
$INPN + OH$	$\rightarrow$	$0.3INO_2 + 0.7HO_2 + 0.7ING_0$	$3.8 \times 10^{-12} \times \exp(200/T)$
$IALD + OH$	$\rightarrow$	$0.430IAO_2 + 0.570IAO_3$	3.7×10^{-11}
$IAO_2 + NO$	$\rightarrow$	OVOC+$0.920HO_2$+$0.920NO_2$+$0.080ING_1$	k_{NO}[b]
$INPN + OH$	$\rightarrow$	$ING_1 + OH$	5×10^{-11}
$ING_1 + OH$	$\rightarrow$	$NO_2 + HO_2$ + OVOC	8×10^{-12}
$ING_2 + OH$	$\rightarrow$	$HO_2 + NO_2$ + OVOC	4×10^{-13}
ING_2	$\rightarrow$	$NO_2 + PA + HO_2$	J_{ING_2}
IAO_2	$\rightarrow$	$CO + MEK + OH$	$k_{=O}^{-H}$[c]
IAO_3	$\rightarrow$	$PACLD + HO_2$	$k_{=O}^{-H}$[c]
MRO_2	$\rightarrow$	$CO + HAC + OH$	$k_{=O}^{-H}$[c]
$ISOPO_2 + HO_2$	$\rightarrow$	ISOPOOH	k_{HO_2}[a]
$ISOPOOH + OH$	$\rightarrow$	$IEPOX + OH$	$1.9 \times 10^{11} \times \exp(390/T)$
$ISOPOOH + OH$	$\rightarrow$	$0.387RIO_2$ + $0.613OH$ + 0.613IALD	$4.75 \times 10^{-12} \exp(200/T)$
PACLD	$\rightarrow$	1.000 OH + 0.500 $(MCO_3 + GLYX + CO + HO_2)$	J_{PACLD}

(a) $k_{HO_2} = 2.91 \times 10^{-13} \exp(1300/\mathrm{T}) (1 - \exp(-0.245 n_C))$ [3]
(b) $k_{NO} = 2.7 \times 10^{-12} \times \exp(350/\mathrm{T})$
(c) $k_{=O}^{-H} = 8.81 \times 10^{9} \exp(-7510/\mathrm{T})$ (Crounse et al., in preparation)
(d) J_{ING_2} estimated using average of cross sections from **(author?)** [2] ; quantum yield estimated by **(author?)** [1]
(e) J_{PACLD} estimated using 2x the cross section of MACR and a quantum yield of 1

References

[1] M. E. Jenkin, S. M. Saunders, and M. J. Pilling. The tropospheric degradation of volatile organic compounds: a protocol for mechanism development. *Atmos. Environ.*, 31(1):81–104, 1997.

[2] James M. Roberts and Ruby W. Fajer. UV absorption cross sections of organic nitrates of potential atmospheric importance and estimation of atmospheric lifetimes. *Environ. Sci. Technol.*, 23(8):945–951, 1989.

[3] S. M. Saunders, M. E. Jenkin, R. G. Derwent, and M. J. Pilling. Protocol for the development of the Master Chemical Mechanism, MCM v3 (Part A): tropospheric degradation of non-aromatic volatile organic compounds. *Atmos. Chem. Phys.*, 3(1):161–180, 2003.